AAS 09-403

# FAILURE-ROBUST THRUSTER COMMANDING FOR SPACE VEHICLES CONTROL

**Fabio Curti,[*] Riccardo Bevilacqua,[†] and Marcello Romano[‡]**

In this paper we study the problem of controlling dynamics of a spacecraft by on-off thrusters only in the case of actuators'failures. We assume that one or more thrusters can fail and that the logic driving the translational and rotational dynamics does not have any information on these events. In particular, the methodology guarantees the Lyapunov-stable tracking of linear models for both the translational and the rotational dynamics of the spacecraft.

## INTRODUCTION

The problem of controlling dynamics of a spacecraft with only the thrusters'actuation is peculiar in the proximity operations such as rendezvous and docking. Such operations are of great interest for future manned missions, on-orbit servicing missions and for the autonomous on-orbit assembly problem[1,2,3,4]. In the case that a thruster fails, there are methods that use failure detection algorithms to guarantee robust controllability of the space vehicle[5,6].

The approach here proposed is based upon a previous work by the authors of this work[7]. In particular, the methodology guarantees Lyapunov-stable tracking of linear models for both the translational and the rotational dynamics of the spacecraft. An on-off command is sent to each thruster, depending on its contribution to the Lyapunov function whose first time derivative must be negative throughout the maneuver. When one or more thrusters fail to turn on, there is still in many cases the capability of controlling the spacecraft since the algorithm keeps selecting thrusters contributing to stabilize the tracking error dynamics. At the moment of a malfunctioning the tracking error increases, thus provoking the remaining actuators to work differently and for longer intervals of firing, in a completely automatic fashion. This means that the algorithm does not know which actuators are failing and it keeps functioning as if they were all active.

The method is experimentally tested on the third generation of spacecraft simulators of the Spacecraft Robotics Lab at the Naval Postgraduate School.

---

[*] Associate Professor, School of Aerospace Engineering-Aerospace and Astronautical Eng. Dept., Via Salaria 851 00138 Rome, Italy (fcurti@psm.uniroma1).
[†] Ph. D., US National Research Council Research Associate, Mechanical and Astronautical Department, Naval Postgraduate School, code AA/RB, Monterey, CA 93940 (rbevilac@nps.edu).
[‡] Assistant Professor, Mechanical and Astronautical Department, Naval Postgraduate School, code MAE/MR 700 Dyer Rd, CA 93940 (mromano@nps.edu)..

## FULLY-ACTUATED SPACECRAFT WITH THRUSTERS ONLY

The roto-translational dynamics of a fully-actuated spacecraft with only thrusters is written here for the three-degree of freedom spacecraft simulator used in the experimental tests. The general equations for a six-degree of freedom space vehicle are found in Reference 7.

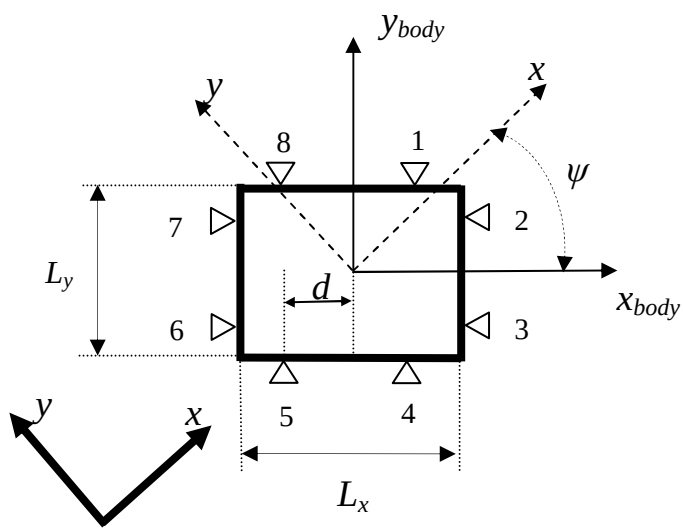


**Figure 1. AMPHIS representative sketch.**

The spacecraft simulator consists of a floating platform, named AMPHIS (Autonomous Multi-Agent Physically Interacting Spacecraft), and a sketch of it is given in Figure 1. A detailed description of the spacecraft simulators, the on-board avionics and the in-door navigation system is given in Reference 8. The frame $(x, y)$ is the Local Reference Frame (LRF), the frame $(x_{body}, y_{body})$ is the Body Reference Frame (BRF), while $\psi$ is the orientation angle of the spacecraft with respect to the LRF; the thrusters are numbered from 1 through 8 and are placed around the platform at a distance of $d$ from the center of mass. The main parameters of AMPHIS are listed in Table 1:

**Table 1. AMPHIS parameters**

| | |
|---|---|
| Mass: | $m = 10.5$ kg |
| Size: | $L_x = 19$ cm; $L_y = 19$ cm |
| Moment of Inertia | $J_z = 0.032\ \mathrm{kg \cdot m^2}$ |
| Thrusters placement: | $d = 5$ cm |
| Thrust: | $u_a = 0.159$ N |
| Minimum impulse duration (valves mechanical limit): | 50 ms |

Let $\underline{\xi} = \begin{bmatrix} x & y & \psi \end{bmatrix}^T$ be the vector of the generalized displacements, the roto-traslational dynamics is:

$$\ddot{\underline{\xi}} = \begin{pmatrix} \frac{1}{m}\,{}^{L}R_B(\psi) & 0_{2\times1} \\ 0_{1\times2} & \frac{1}{J_z} \end{pmatrix} H\,\underline{u} \tag{1}$$

in which $\underline{u} = \begin{bmatrix} u_1 & u_2 & \cdots & u_8 \end{bmatrix}^T$ is the vector of the thrusts of the thrusters with:

$$u_i = \begin{cases} 0 & (i\text{-th thruster OFF}) \\ u_a & (i\text{-th thruster ON}) \end{cases} \qquad i = 1, 2, \cdots 8 \tag{2}$$

where $u_a$ is the positive value of the available thrust. ${}^{L}R_B(\psi)$ is the rotation matrix from the BRF to the LRF:

$${}^{L}R_B(\psi) = \begin{pmatrix} \cos\psi & -\sin\psi \\ \sin\psi & \cos\psi \end{pmatrix} \tag{3}$$

The matrix $H$ is the thrust distribution matrix related to the geometrical structure of the thrusters' placement on the spacecraft. Let ${}^{B}\underline{F}_c$ and ${}^{B}M_c$ be the vectors of control forces and the control torque in the BRF, respectively; then:

$$\begin{bmatrix} {}^{B}\underline{F}_c \\ {}^{B}M_c \end{bmatrix} = \begin{bmatrix} H_F \\ H_M \end{bmatrix} \underline{u} = H\,\underline{u} \tag{4}$$

where:

$$H_F = \begin{bmatrix} 0 & -1 & -1 & 0 & 0 & 1 & 1 & 0 \\ -1 & 0 & 0 & 1 & 1 & 0 & 0 & -1 \end{bmatrix} \tag{5}$$

and:

$$H_M = \begin{bmatrix} -d & d & -d & d & -d & d & -d & d \end{bmatrix} \tag{6}$$

## MODEL-BASED THRUSTERS COMMANDING[7]

The method consists of imposing a reference dynamics that the system must track to make the derivative of a suitable Lyapunov function negative. Let $\underline{\rho} = \begin{bmatrix} x & y \end{bmatrix}^T$ be the position vector; we write the reference dynamics as:

$$\begin{aligned} \ddot{\underline{\rho}}_m + K_1\dot{\underline{\rho}}_m + K_2\underline{\rho}_m &= \underline{v}_{\rho c} \\ \ddot{\psi}_m + k_3\dot{\psi}_m + k_4\psi_m &= v_{\psi c} \end{aligned} \tag{7}$$

where $K_1$ and $K_2$ are $2\times 2$ symmetric positive definite matrices, $k_3 > 0$ and $k_4 > 0$. The variables $\underline{v}_{\rho c}$ and $v_{\psi c}$ are reference commands. If we define the error variables $\underline{\varepsilon}_\rho = \underline{\rho} - \underline{\rho}_m$ and $\varepsilon_\psi = \psi - \psi_m$, we find the equation of the tracking error:

$$\dot{\underline{e}} = A_m\underline{e} + B(\psi)\left(H\underline{u} - \underline{w}\right) \tag{8}$$

where $\underline{e}^T = \begin{bmatrix} \underline{e}_\rho^T & \underline{e}_\psi^T \end{bmatrix}$ with $\underline{e}_\rho^T = \begin{bmatrix} \underline{\varepsilon}_\rho^T & \dot{\underline{\varepsilon}}_\rho^T \end{bmatrix}$, $\underline{e}_\psi^T = \begin{bmatrix} \varepsilon_\rho & \dot{\varepsilon}_\rho \end{bmatrix}^T$ and:

$$A_m = \begin{bmatrix} A_{1m} & 0_{4\times 2} \\ 0_{2\times 4} & A_{2m} \end{bmatrix}, \quad A_{1m} = \begin{bmatrix} 0_{2\times 2} & I_{2\times 2} \\ -K_1 & -K_2 \end{bmatrix}, \quad A_{2m} = \begin{bmatrix} 0 & 1 \\ -k_3 & -k_4 \end{bmatrix} \tag{9}$$

$$B(\psi) = \begin{bmatrix} 0_{2\times 2} & 0_{2\times 1} \\ \frac{1}{m}\,{}^L R_B(\psi) & 0_{2\times 1} \\ 0 & 0 \\ 0 & \frac{1}{J_z} \end{bmatrix}, \quad \underline{w} = \begin{bmatrix} \underline{w}_F \\ w_M \end{bmatrix} = \begin{bmatrix} m\,{}^L R_B(-\psi)\left(\underline{v}_{\rho c} - \underline{v}_{\rho l}\right) \\ J_z\left(v_{\psi c} - v_{\psi l}\right) \end{bmatrix} \tag{10}$$

In Eq. (10) $\underline{v}_{\rho l} = K_1\,\dot{\underline{\rho}} + K_2\,\underline{\rho}$ and $v_{\psi l} = k_3\,\dot{\psi} + k_4\,\psi$. It is noteworthy that if the vector $\underline{w}$ takes the place of the term $H\,\underline{u}$ in Eq.(1), the variables $\underline{w}_F$ and $w_M$ linearize the equation and they force the system to have the dynamics:

$$\begin{aligned} \ddot{\underline{\rho}} + K_1\,\dot{\underline{\rho}} + K_2\,\underline{\rho} &= \underline{v}_{\rho c} \\ \ddot{\psi} + k_3\,\dot{\psi} + k_4\,\psi &= v_{\psi c} \end{aligned} \tag{11}$$

Therefore, the variables $\underline{w}_F$ and $w_M$ are the *ideal controls* for the system in Eq. (1) to yield the behavior of Eq. (7). In fact, in Eq. (8) the term $\left(H\underline{u} - \underline{w}\right)$ forces the dynamics of the tracking error. If this term was zero, the tracking error would go exponentially to zero.

To study the stability of Eq. (8) under the thrusters' actuations, we use the Lyapunov approach by selecting as a candidate function:

$$V\left(\underline{e}\right) = \underline{e}^T P\underline{e} \tag{12}$$

with $P = P^T > 0$. Differentiating Eq. (12) along the trajectories in Eq. (8) we find:

$$\dot{V} = \underline{e}^T \left( A_m P + P A_m^T \right) \underline{e} + 2 \underline{e}^T P \, B(\psi) \left( H \underline{u} - \underline{w} \right) \tag{13}$$

For a given symmetrical positive definite matrix $Q$, the matrix $P$ is found as the unique solution of the Lyapunov equation $A_m P + P A_m^T = -Q$ and Eq. (8) is asymptotically stable if $2 \, \underline{e}^T P \, B(\psi) \left( H \underline{u} - \underline{w} \right) \leq 0$. In particular, if we select:

$$Q = \begin{bmatrix} Q_1 & 0_{4\times 2} \\ 0_{2\times 4} & Q_2 \end{bmatrix} \tag{14}$$

with $Q_1 = Q_1^T > 0$ $4\times 4$-matrix and $Q_2 = Q_2^T > 0$ $2\times 2$-matrix, the solution matrix $P$ has the form[9]:

$$P = \begin{bmatrix} P_\rho & 0_{4\times 2} \\ 0_{2\times 4} & P_\psi \end{bmatrix}, \quad P_\rho = \begin{bmatrix} P_{\rho 1} & P_{\rho 2} \\ P_{\rho 2}^T & P_{\rho 3} \end{bmatrix}, \quad P_\psi = \begin{bmatrix} p_{\psi 1} & p_{\psi 2} \\ p_{\psi 2} & p_{\psi 3} \end{bmatrix} \tag{15}$$

Eq. (13) and Eq. (14) yield:

$$\dot{V} = -\underline{e}_\rho^T \, Q_1 \, \underline{e}_\rho - \underline{e}_\psi^T Q_2 \, \underline{e}_\psi + 2 \, \Delta \tag{16}$$

where, using Eq. (15):

$$\begin{aligned} \Delta &= \Delta_\rho + \Delta_\sigma \\ \Delta_\rho &= \underline{\gamma}_\rho^T \left( H_F \, \underline{u} - \underline{w}_F \right) \\ \Delta_\psi &= \gamma_\psi \left( H_M \, \underline{u} - w_M \right) \\ \underline{\gamma}_\rho^T &= \frac{1}{m} \left( \underline{\varepsilon}_\rho^T P_{\rho 2} + \dot{\underline{\varepsilon}}_\rho^T P_{\rho 3} \right) {}^L R_B(\psi) \\ \gamma_\psi &= \frac{1}{J_z} \left( \varepsilon_\psi \, p_{\psi 2} + \dot{\varepsilon}_\psi \, p_{\psi 3} \right) \end{aligned} \tag{17}$$

Eq. (16) implies that the tracking error $\underline{e} \to \underline{0}$ if $\Delta \leq 0$, that is, by a suitable activation of a set of thrusters. Actually, the tracking error cannot reach zero because in the dynamics of Eq. (1) the control is on-off only. As a consequence, the error reaches a limit cycle whose amplitude is a function of the control parameters $Q$, $K_1$, $K_2$, $k_3$ and $k_4$.

## THRUSTERS' SELECTION STRATEGIES

We seek to establish the asymptotic stability of the reference model tracking error equation Eq. (8) under a suitable selection of the thrusters to be activated. From Eq. (17) we rearrange the two relations:

$$\Delta_\rho = \underline{\beta}_\rho^T \, \underline{\hat{u}} - \delta_F$$
$$\Delta_\psi = \underline{\beta}_\psi^T \, \underline{\hat{u}} - \delta_M \tag{18}$$

with:

$$\underline{\beta}_\rho^T = u_a \, \underline{\gamma}_\rho^T \, H_F, \qquad \underline{\beta}_\psi^T = u_a \, \gamma_\psi \, H_M$$
$$\delta_F = \underline{\gamma}_\rho^T \, \underline{w}_F, \qquad \delta_M = \gamma_\psi \, w_M \tag{19}$$

In Eq. (18) we express the control vector $\underline{u}$ as a function of the binary vector $\underline{\hat{u}}$, that we call *active thrusters' configuration*, for which:

$$\hat{u}_i = \begin{cases} 0 & (i\text{-th thruster OFF}) \\ 1 & (i\text{-th thruster ON}) \end{cases} \qquad i = 1, 2, \cdots 8 \tag{20}$$

and therefore $\underline{u} = u_a \, \underline{\hat{u}}$.

**The *β-strategy***

In this section we recall briefly the strategy we developed in a previous work for the selection of the thrusters to be activated[7]. This strategy is named *β-strategy* because is established on the signs of the vectors' components $\underline{\beta}_\rho^T$ and $\underline{\beta}_\psi^T$. We write the table below, Table 2, where in the first row we put the identification number of the thruster and in the second and third rows the components of the vectors $\underline{\beta}_\rho^T$ and $\underline{\beta}_\psi^T$:

**Table 2. The vectors $\underline{\beta}_\rho^T$ and $\underline{\beta}_\psi^T$.**

| Thruster | 1 | 2 | 3 | 4 | 5 | 6 | 7 | 8 |
|---|---|---|---|---|---|---|---|---|
| $\underline{\beta}_\rho^T$ | $-\varphi_2$ | $-\varphi_1$ | $-\varphi_1$ | $\varphi_2$ | $\varphi_2$ | $\varphi_1$ | $\varphi_1$ | $-\varphi_2$ |
| $\underline{\beta}_\psi^T$ | $-\pi$ | $\pi$ | $-\pi$ | $\pi$ | $-\pi$ | $\pi$ | $-\pi$ | $\pi$ |

where:

$$\varphi_1 = u_a \, \gamma_{\rho 1}; \quad \varphi_2 = u_a \, \gamma_{\rho 2}; \quad \pi = d \, u_a \, \gamma_\psi \tag{21}$$

Note that the functions $\varphi_i$ and $\pi$ can be positive or negative according to the tracking error behavior. If they are all zero, this means that the tracking error is zero. Therefore, the vectors $\underline{\beta}_\rho^T$ and $\underline{\beta}_\psi^T$ have always positive or negative components. Because these components are added in order to give contribution to the derivative of the Lyapunov function (see Eq. (16) and Eq. (18)), the thrusters are selected according to the positions for which the components of the vectors $\underline{\beta}_\rho^T$

and $\underline{\beta}_{\psi}^{T}$ are negative. We assume that the *ideal controls* $w_{F1}$, $w_{F2}$ and $w_M$ satisfy the following conditions:

$$|w_{F1}| \le u_a \; ; \quad |w_{F2}| \le u_a \; ; \quad |w_M| \le 2\, u_a\, d \tag{22}$$

The values of the ideal controls are not known *a priori*, because they are a function of the actual state variables (Eq. (10)) of the system controlled by the thrusters' activations. Assuming the asymptotical stability of Eq. (8), the values of the ideal controls can be predicted by computing $w_{F1}$, $w_{F2}$ and $w_M$ on the reference dynamics of Eq. (11). As a consequence, the control parameters $Q$, $K_1$, $K_2$, $k_3$ and $k_4$, and the reference commands $\underline{v}_{\rho c}$ and $v_{\psi c}$ must be chosen to fulfill the conditions in Eq. (22). These conditions are equivalent to take into account the saturation limits of actuators. From Eq. (14) and Eq. (16) and Table 2, the *β-strategy* is:

1. If $\delta_F \ge 0$ and $\delta_M \ge 0$: no thrusters' activation is needed, because $\Delta$ is not always positive.
2. If $\delta_F < 0$ and $\delta_M \ge 0$: in this case $\Delta_{\psi} \le 0$. We apply the following procedure that generates control forces only and minimizes the number of activated thrusters:
    a. Find the maximum between $|\varphi_1|$ and $|\varphi_2|$. Let $|\varphi_1|$ be the maximum; then the couple of thrusters in the positions $(i, j)$ of Table 2 are selected. The positions $(i, j)$ are where $\varphi_1$ or $-\varphi_1$ appear in Table 2 and for which the components of $\underline{\beta}_{\rho}^{T}$ are negative; therefore, if $\varphi_1 > 0$ the couple is (2,3), that is a force in the opposite direction of the *x-axis*; otherwise the couple is (6,7), that is a force in the direction of the *x-axis*.
    b. Compute $\Delta_{\rho} = \left(\underline{\beta}_{\rho}^{T}\, \underline{\hat{u}} - \delta_F\right)$ with only $\hat{u}_i = 1$ and $\hat{u}_j = 1$ while the others components of $\underline{\hat{u}}$ are set to zero; if $\Delta_{\rho} \le 0$, we stop the procedure, otherwise we would have to activate in addition the couple of thrusters in the positions $(h, k)$ of Table 2 where $\varphi_2$ or $-\varphi_2$ appear and for which the components of $\underline{\beta}_{\rho}^{T}$ are negative; therefore, if $\varphi_2 > 0$ the couple is (1,8), that gives a force in the opposite direction of the *y-axis*; otherwise the couple is (4,5), that gives a force in the direction of the *y-axis*.
3. If $\delta_F \ge 0$ and $\delta_M < 0$: in this case $\Delta_{\rho} \le 0$. We apply the following procedure that generates control torques only and minimizes the number of activated thrusters:
    a. Activate a couple of thrusters in the positions $(i, j)$ of Table 2 for which the components of $\underline{\beta}_{\psi}^{T}$ are negative and no forces are applied. If $\pi > 0$ the couple is (1,5) (or (3,7)), that gives a negative torque; otherwise the couple is (2,6) (or (4,8)), that gives a positive torque.

4. If $\delta_F < 0$ and $\delta_M < 0$: in this case forces and torques must be given at the same time. The procedure is to select the thrusters in the positions where both the component of $\underline{\beta}_\rho^T$ and the component of $\underline{\beta}_\psi^T$ are negative. We apply the following procedure to minimize the number of activated thrusters:

   a. Let $\pi$ be positive. Find the maximum between $|\varphi_1|$ and $|\varphi_2|$. Let $|\varphi_1|$ be the maximum; then if $\varphi_1 > 0$ the thruster $i = 3$ is activated, otherwise the thruster $i = 7$ is activated.

   b. Compute $\Delta = \left(\underline{\beta}_\rho^T \, \underline{\hat{u}} - \delta_F\right) + \left(\underline{\beta}_\psi^T \, \underline{\hat{u}} - \delta_M\right)$ with only $\hat{u}_i = 1$ while the others components of $\underline{\hat{u}}$ are set to zero; if $\Delta \le 0$, we stop the procedure, otherwise in addition we would have to activate the thruster in the position *j* of Table 2, where $j = 1$, if $\varphi_2 > 0$ or $j = 5$, if $\varphi_2 < 0$.

   c. If $\pi$ is negative, we can easily repeat the similar procedure in the items (a) and (b) , in order to find the thrusters to be activated.

The *β-strategy* with the conditions of Eq.(22) ensures that $\Delta \le 0$, and therefore, the tracking error asymptotically reaches the limit cycle.

**Strategy in the presence of thrusters' failures**

The *β-strategy* cannot tolerate failures of the thrusters. To cope with the failures a new thrusters' selection strategy is devised. We define $\underline{\beta} = \underline{\beta}_\rho + \underline{\beta}_\psi$ and $\delta = \delta_F + \delta_M$, and write Table 3 with the same meaning of Table 2.

**Table 3. The *β-vector*.**

| Thruster | 1 | 2 | 3 | 4 | 5 | 6 | 7 | 8 |
|---|---|---|---|---|---|---|---|---|
| $\underline{\beta}^T$ | $-\varphi_2 - \pi$ | $-\varphi_1 + \pi$ | $-\varphi_1 - \pi$ | $\varphi_2 + \pi$ | $\varphi_2 - \pi$ | $\varphi_1 + \pi$ | $\varphi_1 - \pi$ | $-\varphi_2 + \pi$ |

From Eq.(17) and Eq.(18), the thrusters to be activated are those for which:

$$\Delta = \underline{\beta}^T \, \underline{\hat{u}} - \delta \le 0 \tag{23}$$

As a consequence, if $\delta \ge 0$ no thrusters must be activated because Eq.(23) is satisfied with $\underline{\hat{u}} = \underline{0}$. On the contrary, the strategy is to select the thrusters in the positions where the components of the vector $\underline{\beta}$ are negative. Using this approach the following thrusters' selection table is found:

**Table 4. Thrusters'selction table.**

| $\pi$ | $\varphi_1$ | $\varphi_2$ | **No conditions** | | $\lvert\varphi_1\rvert > \lvert\pi\rvert$ | $\lvert\varphi_1\rvert < \lvert\pi\rvert$ | $\lvert\varphi_2\rvert > \lvert\pi\rvert$ | $\lvert\varphi_2\rvert < \lvert\pi\rvert$ |
|---|---|---|---|---|---|---|---|---|
| > 0 | > 0 | > 0 | 3 | 1 | 2 | 7 | 8 | 5 |
| > 0 | < 0 | > 0 | 7 | 1 | 6 | 3 | 8 | 5 |
| > 0 | > 0 | < 0 | 3 | 5 | 2 | 7 | 4 | 1 |
| > 0 | < 0 | < 0 | 7 | 5 | 6 | 3 | 4 | 1 |
| < 0 | > 0 | > 0 | 2 | 8 | 3 | 6 | 1 | 4 |
| < 0 | < 0 | > 0 | 6 | 8 | 7 | 2 | 1 | 4 |
| < 0 | > 0 | < 0 | 2 | 4 | 3 | 6 | 5 | 8 |
| < 0 | < 0 | < 0 | 4 | 6 | 7 | 2 | 5 | 8 |
| *Failure variables* | | | $f_{n1}$ | $f_{n2}$ | $f_{c1}$ | | $f_{c2}$ | |

According to the signs of the functions $\varphi_1$, $\varphi_2$ and $\pi$, in Table 3 we indentify the positions for which the components of the vector $\underline{\beta}$ are negative. These positions are related to thrusters to be activated with no conditions as shown in Table 4. Moreover, under the conditions on the functions $\varphi_1$, $\varphi_2$ and $\pi$ of Table 4, additional thrusters are selected.

As an example, the first row of Table 4 states that thrusters 1 and 3 are activated. Assuming that $\lvert\varphi_1\rvert > \lvert\pi\rvert$ and $\lvert\varphi_2\rvert < \lvert\pi\rvert$, the thrusters 2 and 5 are activated as well. Looking the thruster's placement in Figure 1, this is equivalent to have a negative torque and a force in the opposite direction of the *x-axis*. Because the functions $\varphi_1$, $\varphi_2$ and $\pi$ are positive or negative, and, $\lvert\varphi_k\rvert > \lvert\pi\rvert$ or $\lvert\varphi_k\rvert < \lvert\pi\rvert$, four thrusters are always selected. These thrusters give the simultaneous combination of torques and forces to control the spacecraft. Now, we include in the strategy the presence of failures. We introduce the *failure variables* $f_{n1}$, $f_{n2}$, $f_{c1}$ and $f_{c2}$. If no failures occur all these variables are zero, otherwise from Table 4:

- $f_{n1} = 1$ a failure occurs on the first selected thruster in the *no-conditions* column;
- $f_{n2} = 1$ a failure occurs on the second selected thruster in the *no-conditions* column;
- $f_{c1} = 1$ a failure occurs on the selected thruster in the column related to $\varphi_1$;
- $f_{c2} = 1$ a failure occurs on the selected thruster in the column related to $\varphi_2$;

From Eq. (19) and Table 4, for all the cases listed in the table Eq. (23) yields:

$$\Delta = -\left(|\varphi_1| + |\pi|\right)\cdot\left(1 - f_{n1}\right) - \left(|\varphi_2| + |\pi|\right)\cdot\left(1 - f_{n2}\right) - \left||\varphi_1| - |\pi|\right|\cdot\left(1 - f_{c1}\right) + \\ -\left||\varphi_2| - |\pi|\right|\cdot\left(1 - f_{c2}\right) - \gamma_{\rho 1}\, w_{F1} - \gamma_{\rho 2}\, w_{F2} - \gamma_{\psi}\, w_M \tag{24}$$

As stated above, if $\delta < 0$ thrusters must be selected. The worst case is when $\delta$ has the most negative values that occurs when at the same time $\gamma_{\rho 1}\, w_{F1} < 0$, $\gamma_{\rho 2}\, w_{F2} < 0$ and $\gamma_{\psi}\, w_M < 0$. Therefore, in this case Eq. (23) becomes:

$$\tilde{\Delta} = -\left(|\varphi_1| + |\pi|\right)\cdot\left(1 - f_{n1}\right) - \left(|\varphi_2| + |\pi|\right)\cdot\left(1 - f_{n2}\right) - \left||\varphi_1| - |\pi|\right|\cdot\left(1 - f_{c1}\right) + \\ -\left||\varphi_2| - |\pi|\right|\cdot\left(1 - f_{c2}\right) + \left|\gamma_{\rho 1}\right|\left|w_{F1}\right| + \left|\gamma_{\rho 2}\right|\left|w_{F2}\right| + \left|\gamma_{\psi}\right|\left|w_M\right| \tag{25}$$

By using Eq. (21), Eq. (25) yields:

$$\tilde{\Delta} = \left|\gamma_{\rho 1}\right|\cdot\left(-u_a + \left|w_{F1}\right|\right) + \left|\gamma_{\rho 2}\right|\cdot\left(-u_a + \left|w_{F2}\right|\right) + \left|\gamma_{\psi}\right|\left(-2\, u_a\, d + \left|w_M\right|\right) + \\ + u_a\left(\left|\gamma_{\rho 1}\right| + d\left|\gamma_{\psi}\right|\right)\cdot f_{n1} + u_a\left(\left|\gamma_{\rho 2}\right| + d\left|\gamma_{\psi}\right|\right)\cdot f_{n2} + \\ + u_a\left|\left|\gamma_{\rho 1}\right| - d\left|\gamma_{\psi}\right|\right|\cdot f_{c1} + u_a\left|\left|\gamma_{\rho 2}\right| - d\left|\gamma_{\psi}\right|\right|\cdot f_{c2} - r \tag{26}$$

where:

$$r = u_a\left|\left|\gamma_{\rho 1}\right| - d\left|\gamma_{\psi}\right|\right| + u_a\left|\left|\gamma_{\rho 2}\right| - d\left|\gamma_{\psi}\right|\right| \tag{27}$$

Eq. (26) shows that if the conditions of Eq. (22) hold, $\tilde{\Delta}$ is upper bounded by the following expression:

$$\tilde{\Delta} \le u_a\left(\left|\gamma_{\rho 1}\right| + d\left|\gamma_{\psi}\right|\right)\cdot f_{n1} + u_a\left(\left|\gamma_{\rho 2}\right| + d\left|\gamma_{\psi}\right|\right)\cdot f_{n2} + \\ + u_a\left|\left|\gamma_{\rho 1}\right| - d\left|\gamma_{\psi}\right|\right|\cdot f_{c1} + u_a\left|\left|\gamma_{\rho 2}\right| - d\left|\gamma_{\psi}\right|\right|\cdot f_{c2} - r \tag{28}$$

From Eq. (28), if no failures occur that $\tilde{\Delta} < 0$ because $\Delta \le \tilde{\Delta}$ and the stability of Eq. (8) is ensured. We demonstrate in the next section how the strategy supports failures keeping the tracking error dynamics stable.

## FAILURE-TOLERANT BETA-STRATEGY

The above designed strategy is based on the signs and the values of the components of the vector $\underline{\beta}$ of Table 3; we analyze the cases in which one or more failures occur. Table 4 helps us in the following.

### One Thruster-Failure

If one failure of type $f_{ck}$ occurs, from Eq. (28) and Eq. (29) yield $\tilde{\Delta} < 0$. Assume a failure of type $f_{nk}$, we have from Eq. (16):

$$\dot{V} \le -\lambda_m\left(Q_1\right)\left\|\underline{e}_\rho\right\|^2 - \lambda_m\left(Q_2\right)\left\|\underline{e}_\psi\right\|^2 + 2\,u_a\left|\gamma_{\rho k}\right| + 2\;u_a\;d\left|\gamma_\psi\right| - 2\,r \tag{30}$$

where $\lambda_m\left(Q_1\right)$ and $\lambda_m\left(Q_2\right)$ are the minimum eigenvalues of $Q_1$ and $Q_2$, respectively, that are positive. From Eq. (17) we can write:

$$\begin{aligned} \underline{\gamma}_\rho &= {}^L R_B\left(-\psi\right) K_\rho\, \underline{e}_\rho \\ \gamma_\psi &= k_\psi^T\, \underline{e}_\psi \end{aligned} \tag{31}$$

where $K_\rho = 1/m \cdot \left[P_{\rho 2} \quad P_{\rho 3}\right]$ and $k_\psi^T = 1/J_z \cdot \left[p_{\psi 2} \quad p_{\psi 3}\right]$. As a consequence, we find:

$$\begin{aligned} &\left(\left|\gamma_{\rho 1}\right|^2 + \left|\gamma_{\rho 2}\right|^2\right)^{\frac{1}{2}} \le \sigma_M\left(K_\rho\right)\left\|\underline{e}_\rho\right\| \\ &\left|\gamma_\psi\right| \le \left\|k_\psi\right\| \cdot \left\|\underline{e}_\psi\right\| \end{aligned} \tag{32}$$

in which $\sigma_M\left(K_\rho\right)$ is the maximum singular value of $K_\rho$. The first equation of Eq. (32) states that the pair of values $\left|\gamma_{\rho 1}\right|$, $\left|\gamma_{\rho 2}\right|$ belongs to the set shown in Figure 2.

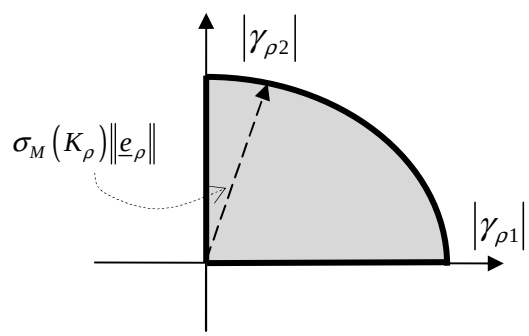


**Figure 2.** $\left|\gamma_{\rho 1}\right|$ **and** $\left|\gamma_{\rho 2}\right|$ **boundaries.**

Therefore we can take the upper bound $\left|\gamma_{\rho k}\right| < \sigma_M\left(K_\rho\right)\left\|\underline{e}_\rho\right\|$ (with $k = 1$ or $k = 2$) and Eq. (30) becomes:

$$\dot{V} < -\alpha_1 - \alpha_2 - 2\,r \tag{33}$$

where:

$$\alpha_1 = \lambda_m\left(Q_1\right)\left\|\underline{e}_\rho\right\|^2 - 2\,u_a\,\sigma_M\left(K_\rho\right)\left\|\underline{e}_\rho\right\|$$
$$\alpha_2 = \lambda_m\left(Q_2\right)\left\|\underline{e}_\psi\right\|^2 - 2\,d\,u_a\left\|k_\psi\right\|\cdot\left\|\underline{e}_\psi\right\| \tag{34}$$

If the variables $\alpha_1$ and $\alpha_2$ are not negative, the derivative of the Lyapunov function is upper bounded with a negative value. This happens when:

$$\left\|\underline{e}_\rho\right\| \geq \frac{2\,u_a\sigma_M\left(K_\rho\right)}{\lambda_m\left(Q_1\right)}, \quad \left\|\underline{e}_\psi\right\| \geq \frac{2\,d\,u_a\left\|k_\psi\right\|}{\lambda_m\left(Q_2\right)} \tag{35}$$

When a failure occurs the tracking error can increase, but after a threshold the derivative of the Lyapunov function becomes negative and the tracking error does no longer increase. Note that even if the derivative of the Lyapunov equation is not negative, it does not imply that the tracking error dynamics is not stable. Therefore, even if $\dot{V} \geq 0$ the tracking error can be bounded.

Eq. (35) gives a simple numerical test to verify if the assumptions on $w_{F1}$, $w_{F2}$ and $w_M$ in Eq.(22) hold. In fact, the values of $w_{F1}$, $w_{F2}$ and $w_M$ are predicted on the reference dynamics. Therefore, the smaller the lower bound in Eq. (35) is, the fewer the actual dynamics moves away from the reference dynamics, and as a result $\left|w_{F1}\right| \leq u_a$ , $\left|w_{F2}\right| \leq u_a$ and $\left|w_M\right| \leq 2\,u_a\,d$ .

**Two Thruster-Failures**

If the two thruster-failures are of type $f_{ck}$ the condition $\tilde{\Delta} < 0$ holds. For one failure of type $f_{ck}$ type and one of type $f_{nk}$, the derivative of the Lyapunov function is upper bounded as:

$$\dot{V} < -\alpha_1 - \alpha_2 - r \tag{36}$$

For two failures of $f_{nk}$ type, from Eq. (16) and Eq.(28) we have:

$$\dot{V} \leq -\lambda_m\left(Q_1\right)\left\|\underline{e}_\rho\right\|^2 - \lambda_m\left(Q_2\right)\left\|\underline{e}_\psi\right\|^2 + 2u_a\left|\gamma_{\rho 1}\right| + 2\,u_a\left|\gamma_{\rho 2}\right| + 4u_a\,d\left|\gamma_\psi\right| - 2\,r \tag{37}$$

Using the first equation of Eq. (32), and looking Figure 2, we have $\left|\gamma_{\rho 1}\right| + \left|\gamma_{\rho 2}\right| \leq \sqrt{2}\,\sigma_M\left(K_\rho\right)\left\|\underline{e}_\rho\right\|$, and as a consequence:

$$\dot{V} < -\alpha'_1 - \alpha'_2 - 2\,r \tag{38}$$

where:

$$\alpha'_1 = \lambda_m(Q_1)\left\|\underline{e}_\rho\right\|^2 - 2\sqrt{2}\,u_a\sigma_M\left(K_\rho\right)\left\|\underline{e}_\rho\right\|$$
$$\alpha'_2 = \lambda_m(Q_2)\left\|\underline{e}_\psi\right\|^2 - 4\,u_a\,d\left\|k_\psi\right\|\left\|\underline{e}_\psi\right\| \tag{39}$$

which implies:

$$\left\|\underline{e}_\rho\right\| \geq \frac{2\sqrt{2}\,u_a\sigma_M\left(K_\rho\right)}{\lambda_m(Q_1)}; \qquad \left\|\underline{e}_\psi\right\| \geq \frac{4\,u_a\,d\left\|k_\psi\right\|}{\lambda_m(Q_2)} \tag{40}$$

As in the previous case, the lower bounds of Eq. (40) help us verify the assumptions on the *ideal controls* $w_{F1}, w_{F2}$ and $w_M$ .

**Three or Four Thruster-Failures**

The strategy is able to cope with more than two thruster-failures. For three thruster-failures the derivative of the Lyapunov is upper bounded by:

$$\dot{V} < -\alpha_1 - \alpha_2 \tag{41}$$

if there are two failures of type $f_{ck}$ and one of type $f_{nk}$. On the contrary, two failures of type $f_{nk}$ and one of type $f_{ck}$, the upper bound is:

$$\dot{V} < -\alpha'_1 - \alpha'_2 - r \tag{42}$$

For four thruster-failures we obtain:

$$\dot{V} < -\alpha'_1 - \alpha'_2 \tag{43}$$

The result is that if $\alpha'_1 \geq 0$ and $\alpha'_2 \geq 0$ the method guarantees that $\dot{V} < 0$ and the tracking error dynamics is asymptotically stable.

**Controllability in the presence of Thruster-Failures**

The analysis has shown that the strategy is able to manage up to four failures. Actually, some sets of thrusters cannot fail at the same time. As an example from Figure 1, if thruster 1 and thruster 8 fail at the same time, we lose the controllability along the negative direction of the *y-axis*. If thrusters 1, 3, 5 and 7 fail, we cannot apply a positive torque. Therefore, to keep the controllability of the system some failures are not allowed, as listed in Table 5:

**Table 5. Critical failures.**

| Thrusters | Actuation lost |
|---|---|
| 1 8 | *Force –y* |
| 2 3 | *Force -x* |
| 4 5 | *Force x* |
| 6 7 | *Force y* |
| 1 3 5 7 | *Torque <0* |
| 2 4 6 8 | *Torque >0* |

## EXPERIMENTAL RESULTS

This section reports the results of two experimental tests performed by implementing the *failure-tolerant β-strategy* on board of one AMPHIS. The robot starts maneuvering from the initial state vector

$$\begin{bmatrix} x_0 & y_0 & \psi & \dot{x}_0 & \dot{y}_0 & \omega \end{bmatrix} = \begin{bmatrix} 0\,m & 1\,m & 0\,\text{deg} & 0\,{}^{m}\!/_{s} & 0\,{}^{m}\!/_{s} & 0\,{}^{\text{deg}}\!/_{s} \end{bmatrix} \tag{43}$$

and it is intended to track a one meter radius circular trajectory at constant speed, while changing its attitude between 30 and -30 degrees following a sine wave command. The commanded trajectory's frequency is $\varpi_\rho = 0.025\,{}^{rad}\!/_{\text{sec}}$, the angle's command frequency is $\varpi_\psi = 0.05\,{}^{rad}\!/_{\text{sec}}$. This means that the circle is intended to be run in approximately 250 seconds while the angle's oscillation between 30 and -30 degrees occurs twice within the same time frame. Therefore the reference commands (Eq. (7)) have the expressions:

$$\begin{aligned} \underline{v}_{\rho c} &= \ddot{\underline{\rho}}_c + K_1\,\dot{\underline{\rho}}_c + K_2\,\underline{\rho}_c \\ v_{\psi c} &= \ddot{\psi}_c + k_3\,\dot{\psi}_c + k_4\,\psi_c \end{aligned} \tag{44}$$

where $\underline{\rho}_c^T = \begin{bmatrix} \cos(\varpi_\rho\, t) & \sin(\varpi_\rho\, t) \end{bmatrix}$ and $\psi_c = 0.5233\cos(\varpi_\psi\, t)$.

In the first test the robot has no thruster-failures, while in the second test thrusters 1, 2 and 6 fail after 90 s from the start time. The gains of the reference dynamics of Eq. (7) are:

$$K_1 = 10.6 \cdot I_{2\times2}, \quad K_2 = 35.13 \cdot I_{2\times2}, \quad k_3 = 0.24\,, \quad k_4 = 0.5 \tag{45}$$

while the matrices used in the Lyapunov equation are:

$$Q_1 = 5 \cdot I_{2\times2}, \quad Q_2 = 50 \cdot I_{2\times2} \tag{46}$$

### Experimental Test 1: No Failures

Figure 3 shows the snapshots of the robot during the tracking of the commanded trajectory. The bolded side of the square is used to visualize the heading of the spacecraft simulator.

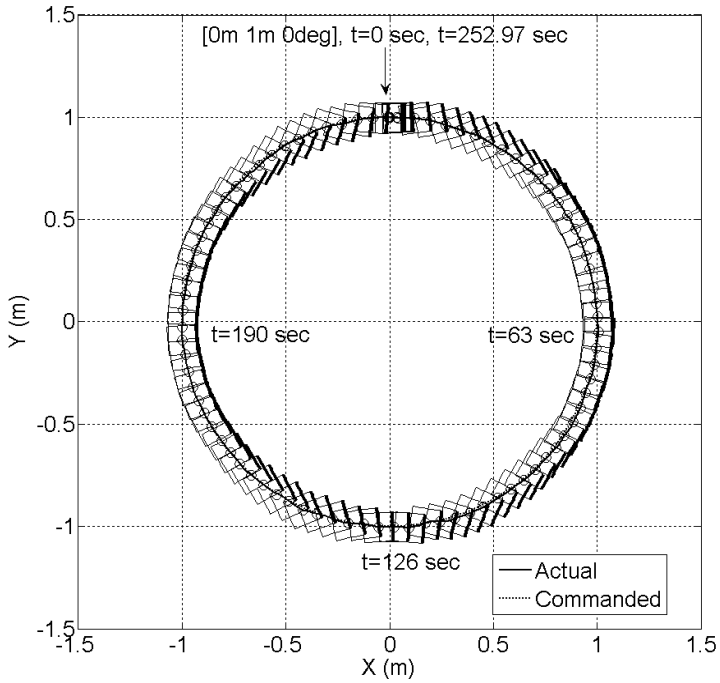


**Figure 3. Experimental Results: Bird's Eye View for No Failures Trajectory Tracking.**

The behaviors of the tracking errors are depicted in Figure 4. The results show that the position errors are kept within 1 cm for $x$ and within 2cm for $y$. The attitude parameter $\psi$ is tracking the maneuver with the accuracy of 0.5 deg.

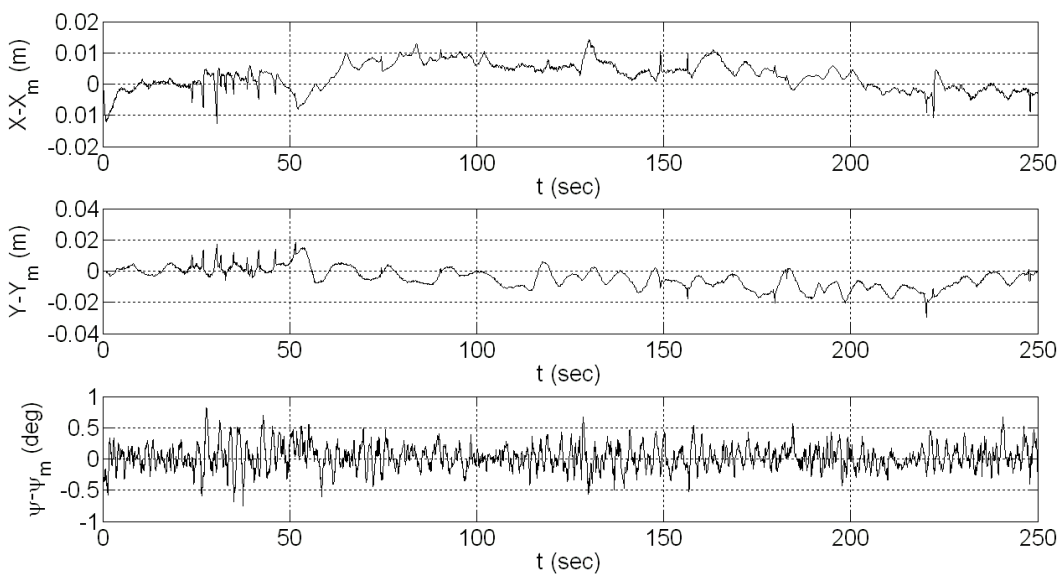


**Figure 4. Experimental Results: $x, y$ and $\psi$ Tracking Errors.**

**Experimental Test 2: Failure in the Thrusters 1, 2 and 6**

Using Eq. (44) and (45) we find $\sigma_M\left(K_\rho\right)=0.0237$ and $\left\|k_\psi\right\|=30.98$, while $\lambda_m\left(Q_1\right)=5$ and $\lambda_m\left(Q_2\right)=50$. Now, we compute the bounds of Eq. (39) :

$$\left\|\underline{e}_\rho\right\| \geq \frac{2\sqrt{2}\,u_a\sigma_M\left(K_\rho\right)}{\lambda_m\left(Q_1\right)}=2.13\cdot 10^{-3}; \qquad \left\|\underline{e}_\psi\right\| \geq \frac{4\,u_a\,d\left\|k_\psi\right\|}{\lambda_m\left(Q_2\right)}=1.97\cdot 10^{-2} \tag{46}$$

Therefore, from a theoretical point of view, we expect that the strategy can manage the thrusters' failures.

In Figure 5 we find the snapshots of the robot during the maneuvers and it is shown the point where the three failures occur at the same time. The behavior of the tracking error is given in Figure 6 and the increasing error is clearly visible after the malfunctioning. This affects the *x-component* of the position more than the other displacements' variables, but the strategy is able to recovery the increased error. Figure 7 shows the history of the thrusters' commands during the robot maneuvers.

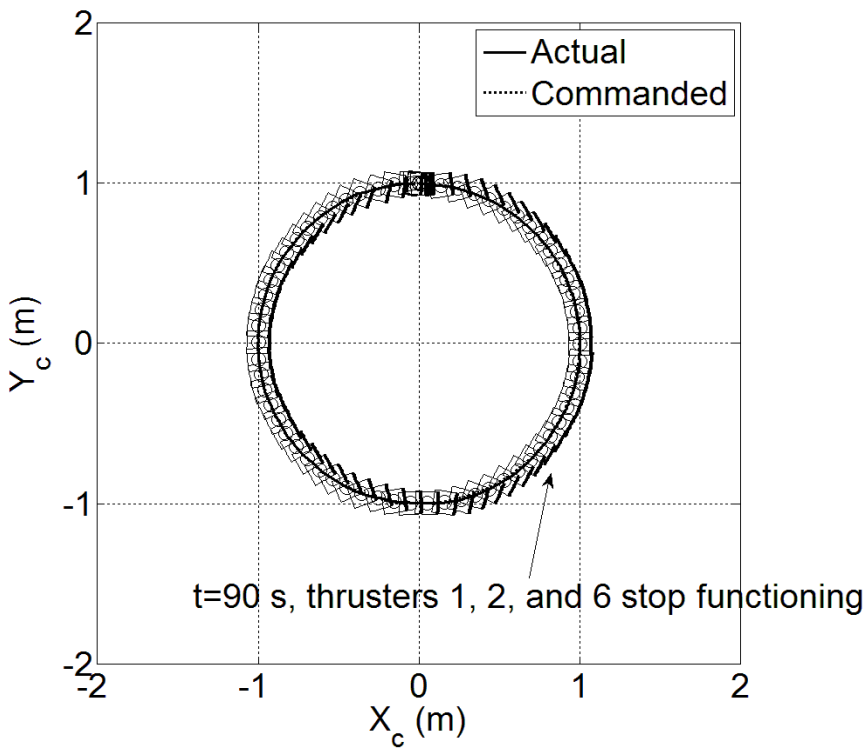


**Figure 5. Experimental Results: Bird's Eye View with Three Thruster-Failures.**

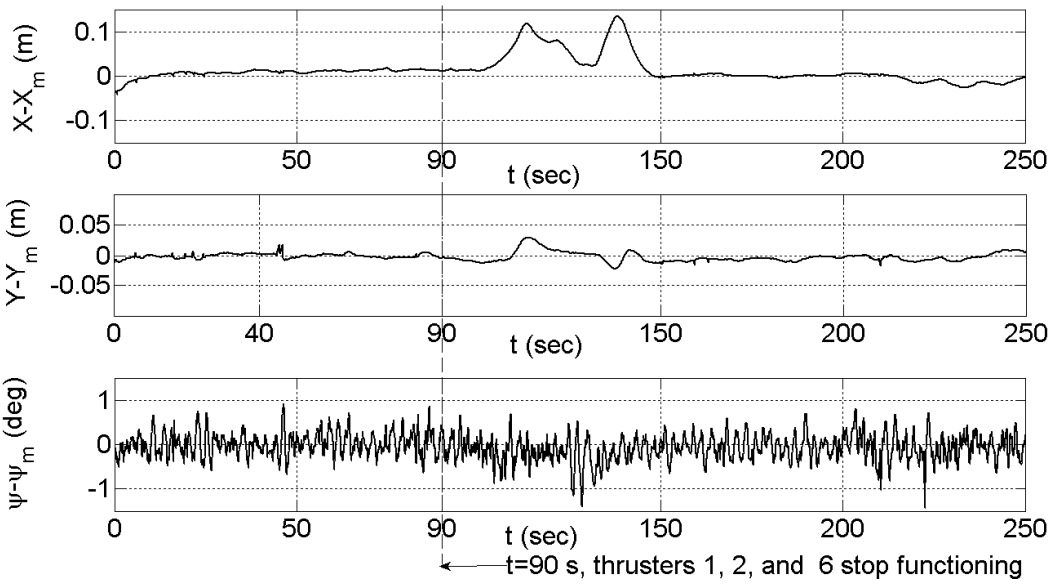


**Figure 6. Experimental Results: $x, y$ and $\psi$ Tracking Errors with Three Thruster-Failures.**

## CONCLUSION

The paper has presented a failure-tolerant thrusters' commanding strategy for controlling translational and rotational dynamics of fully-actuated spacecraft with thrusters only. In particular the analysis has focused on the control problem of the spacecraft simulator AMPHIS of the Spaceraft Robotics Lab of the Naval Postgraduate School.

It has been demonstrated in this work that the method is able to compensate up to four thrusters' failures. The experimental tests have compared the behavior of AMPHIS, accomplishing commanded tasks, in the case of no failures and when three failures occur. The experimental results have shown that the tracking errors increase after the failures' event, but the strategy recovers the malfunctioning and reduces the tracking errors.

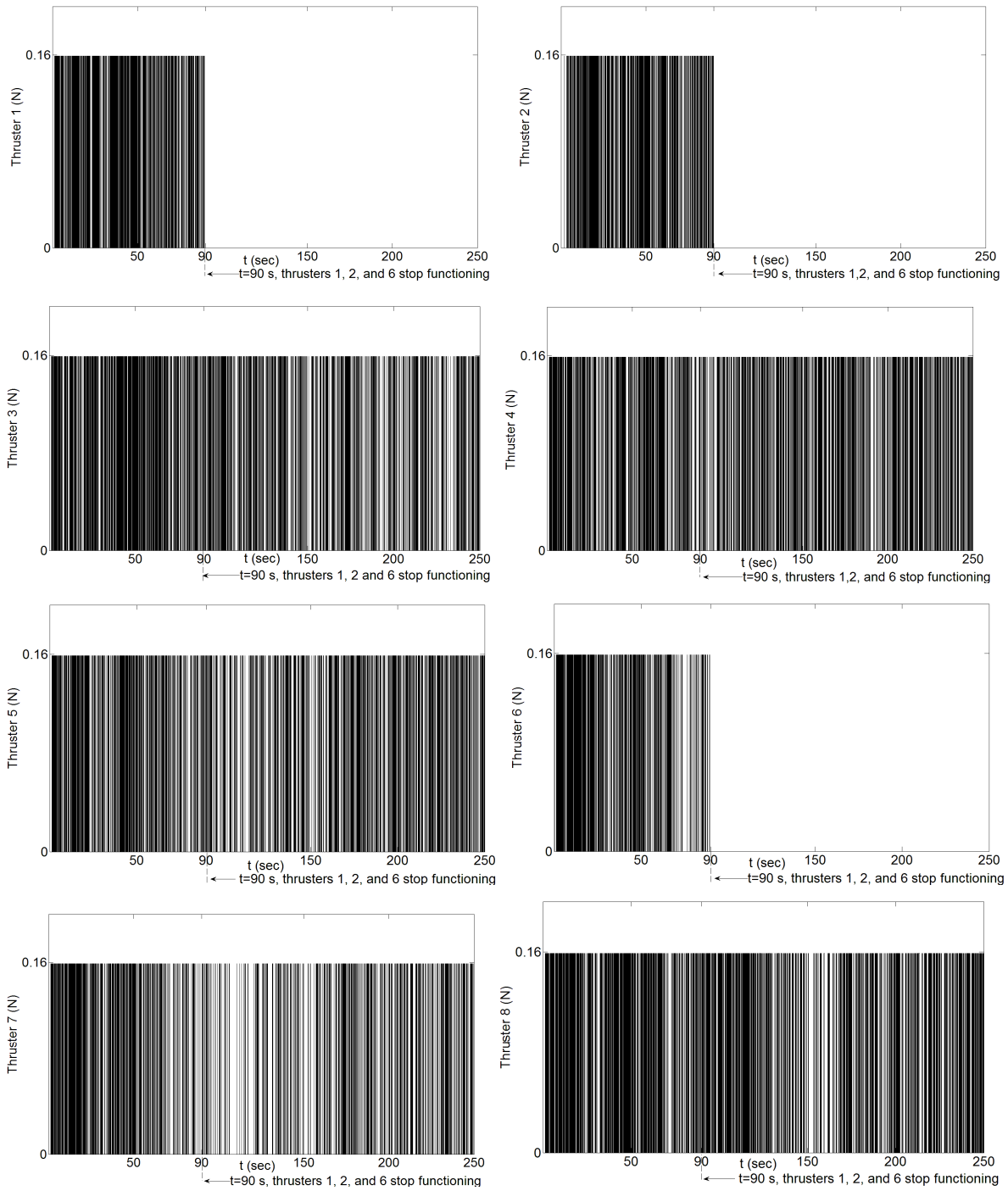


**Figure 7. Experimental Results: Thrusters' Commands History with Three Failures.**

**NOTATION**

| | | |
|---|---|---|
| $\alpha_1, \alpha_2, \alpha'_1, \alpha'_2$ | = | Terms in the upper bounds of the derivative of the Lyapunov function |
| $\underline{\beta}_\rho, \underline{\beta}_\psi, \underline{\beta}$ | = | Vectors of the Thrusters' selection |
| $\delta, \delta_F, \delta_M$ | = | Activation variables |
| $\underline{\varepsilon}_\rho$ | = | Position tracking error vector |
| $\underline{\varepsilon}_\psi$ | = | Attitude tracking error vector |
| $\varphi_1, \varphi_2, \pi$ | = | Switching variables |
| $\lambda$ | = | Eigenvalue |
| $\omega$ | = | Angular velocity |
| $\varpi$ | = | Command frequency |
| $\psi$ | = | Attitude angle |
| $\underline{\rho}$ | = | Position vector |
| $\sigma$ | = | Singular eigenvalue |
| $\Delta$ | = | Term of the time derivative of the Lyapunov function |
| $\underline{e}_\rho$ | = | Tracking error vector of the translational dynamics |
| $\underline{e}_\psi$ | = | Tracking error vector of the rotational dynamics |
| $f_{n1}, f_{n2}, f_{c1}, f_{c2}$ | = | Binary variables representing failures |
| $k_3, k_4, k_\psi$ | = | Gain coefficients |
| $\underline{u}$ | = | Vector of the activated thrusters |
| $\underline{\hat{u}}$ | = | Binary vector of the activated thrusters |
| $u_a$ | = | Thrust of a thruster |
| $w_{F1}, w_{F2}, w_M$ | = | Ideal controls |
| $A_m$ | = | Model reference dynamics matrix |

| | | |
|---|---|---|
| $B(\psi)$ | = | Control distribution matrix |
| $H, H_F, H_M$ | = | Thrust distribution matrices |
| $K_1, K_2, K_\rho$ | = | Gain matrices |
| $P, P_\rho, P_\psi$ | = | Lyapunov matrices |
| $Q_1, Q_2, Q$ | = | Positive definite matrices |
| $V$ | = | Lyapunov function |

## REFERENCES


[1]Jackson, M., Gonzales, R., "Orion Orbit Reaction Control Assessment," AIAA Guidance, Navigation and Control Conference and Exhibit, 20-23 August 2007, Paper 2007-6684.

[2]Subbarao, K., Weish, S., "Nonlinear Control of Motion Synchronization for Satellite Proximity Operations," *Journal of Guidance, Control and Dynamics*, Vol. 31, No. 5. Sept-Oct. 2008, pp. 1284-1292

[3]Luo, Y.Z., Tang, G.J., and Lei, Y.J., "Optimal Multi-Objective Linearized Impulsive Rendezvous," *Journal of Guidance, Control, and Dynamics*, Vol. 30, No. 2, March-April 2007, pp. 383-389.

[4]Badawy, A., McInnes, C.R., "On-orbit assembly using superquadric potential field," *Journal of Guidance, Control and Dynamics*, Vol. 31, No. 1. Jan.-Feb. 2008, pp. 30-43.

[5]Augustin, R.,M., Mangoubi, R., S., Hain, R., M., Adams, N., J., "Robust Failure Detection for Reentry Vehicle Attitude Control Systems," *Journal of Guidance, Control, and Dynamics*, Vol. 22, No. 6, pp.839-845, 1999.

[6]Yang, T., "Optimal Thruster Selection with Robust Estimation for Formation Flying Applications," M. Sc. Thesis in Aeronautics and Astronautics, MIT, 2003

[7]Curti, F., Romano, M., Bevilacqua, R., "Model Based Thruster Commanding for Rotational and Translational Control of a Spacecraft", submitted for publication.

[8]Bevilacqua, R., Hall, J., Horning, J., Romano, M., "Ad-hoc Wireless Networking and Shared Computation based upon Linux for Autonomous Multi-Robot Systems," *AIAA Journal of Aerospace Computing, Information, and Communication*, 2009 1542-9423 vol.6 no.5 (328-353)

[9]Gantmacher, F.R, *Matrix Theory Vol. 1*, American Mathematical Society, 2000